# A state-compensation extended state observer for model predictive control

Liu, Chenguang; Negenborn, Rudy R.; Zheng, Huarong; Chu, Xiumin

**DOI**
10.1016/j.ejcon.2017.05.002

**Publication date**
2017

**Document Version**
Final published version

**Published in**
European Journal of Control

European Journal of Control 36 (2017) 1–9

Contents lists available at ScienceDirect

European Journal of Control

journal homepage: www.elsevier.com/locate/ejcon

# A state-compensation extended state observer for model predictive control

Chenguang Liu [a,b,*], Rudy R. Negenborn [b], Huarong Zheng [b], Xiumin Chu [a]

[a] *National Engineering Research Center for Water Transport Safety, Wuhan University of Technology, Wuhan, PR China*
[b] *Department of Maritime and Transport Technology, Delft University of Technology, Delft, The Netherlands*

ARTICLE INFO

*Article history:*
Received 7 December 2016
Revised 21 March 2017
Accepted 1 May 2017
Available online 8 May 2017

Recommended by A. Zemouche.

*Keywords:*
Extended state observer
Model predictive control
Discrete-time control
Ship motion model

ABSTRACT

Motion control in absence of human involvement is difficult to realize for autonomous vessels because there usually exist environmental disturbances and unmeasurable states at the same time. A discrete-time model predictive control (MPC) approach based on a state-compensation extended state observer (SCESO) is proposed to achieve more precise control performance with state estimations and disturbance rejections simultaneously. The main idea is that lumped disturbances encompassing nonlinear dynamics and external disturbances are handled as two parts, unlike the standard extended state observer (ESO). Particularly, the nonlinear terms are compensated by estimated states and the external disturbances are considered as extended states and attenuated by the traditional ESO strategy. Assuming that the lumped disturbances are constant over the prediction horizon, the prediction model is linearized to save computational time since after linearization the online MPC optimization problems are solved as quadratic programming problems instead of nonlinear programming problems. The convergence of the proposed SCESO estimation errors to zero is proved even when the disturbances keep variable. Two case studies involving a numerical example and ship heading control have been conducted to verify the effectiveness of the proposed control method.



## 1. Introduction

In a real system, there usually exist external disturbances, nonlinear dynamics, and unmeasurable states that bring challenges to the controller design for such a system [6,19,41,42]. Autonomous vessels have been encountering these challenges in motion control, e.g., path following or trajectory tracking [20,45], because wind, current or waves always exist and heading acceleration is hardly measured directly [26]. To obtain reliable performance, a controller needs to reject the effect of disturbances and use as precise as possible state information. Observers are often utilized to estimate states or disturbances that are unknown. For the estimation of states, state observers, e.g., Luenberger observers [43], Kalman filter-based estimators [35], and sliding observers [31], have been used widely. For the estimation of disturbances, disturbance observers (DOB) have been developed and applied in industry [5,41]. A review of DOB-based control (DOBC) methods can be found in [6]. Generally, states and disturbances need to be estimated at the same time. Unknown input observers (UIO) [4,15], and extended state observers (ESO) [13,14], can deal with state and disturbance estimation problems simultaneously [15]. UIO has been used widely in fault diagnosis and isolation [4,27,28,37]. ESO was first proposed for active disturbance rejection control by Han [13]. After that, ESO has been used and discussed widely with applications of active disturbance rejection control [11,30,32,33]. ESO is actually the same as UIO if the assumptions of disturbances for UIO and ESO are consistent [6].

Different from most existing observers, the ESO adds another state to a system instead of reducing the system order [38] and requires the least amount of system information [46]. ESO-based control has also been applied as composite control combined with feedback and disturbance compensation [19], predictive functional control [21], and sliding mode control [39]. Moreover, the ESO itself has been improved both in the aspects of practical applications and theories. A linear ESO method was presented to simplify the implementation of ESO for engineers in [9]. For a rigorous proof of the ESO convergence, a high gain approach was used to eliminate the influence of uncertainties for nonlinear extended state observers [12]. Furthermore, an extended high-gain state observer was proposed to deal with a class of nonlinear uncertain systems in which known nonlinear terms were used in the observer design [8]. A generalized ESO was represented to deal with a system

* Corresponding author.
*E-mail addresses:* liuchenguang@whut.edu.cn (C. Liu), R.R.Negenborn@tudelft.nl (R.R. Negenborn), H.Zheng-1@tudelft.nl (H. Zheng), chuxm@whut.edu.cn (X. Chu).

http://dx.doi.org/10.1016/j.ejcon.2017.05.002

model that did not satisfy the standard chain form [19]. However, there are some defects for ESO. For instance, the ESO estimated errors cannot be guaranteed to converge to zero unless under the assumptions that the disturbances are constant [19]. Generally, the errors can only be guaranteed to be within the vicinity of zero with bounded disturbances [9,12].

Model predictive control (MPC) is an important advanced control method in industrial areas due to its optimized control performance and the ability of considering various kinds of constraints explicitly [22,42]. An MPC based controller relies on state measuring, disturbance estimating and an accurate prediction model [47]. DOB based MPC methods have been developed and proved to be effective by compensating the effect of unknown disturbances and uncertainties recently [18,40–42,47]. Considering that the ESO is a combination of DOB and state observer, it is reasonable to utilize the ESO to estimate unmeasurable or costly-measured states and unknown disturbances at the same time for a MPC based controller. A simplified MPC method, i.e., predictive functional control (PFC), is employed with the ESO for speed control of permanent magnet synchronous motor servo system [21]. One deficiency of the proposed method in [21] is that the ESO based feedforward control law is designed separately and is not taken into account in the receding optimization process of PFC. Another deficiency is that there is no strict proof of the convergence of ESO estimation errors [41]. Note that MPC is usually implemented as a digital control because an analog circuit hardly deals with online linear programming, quadratic programming, or nonlinear programming problems [36]. For the digital control, system and observer models should be discretized and the control input should be updated during the sampling interval [7].

In this article, an improved ESO based MPC approach for a discrete-time prediction model is proposed to achieve more precise control performance while estimating states and rejecting disturbances. The main idea is that lumped disturbances encompassing nonlinear dynamics and external disturbances are handled separately, which is different from the standard ESO. In this method, the nonlinear terms are compensated by estimated states, and external disturbances are considered as extended states and estimated by the proposed ESO. The lumped disturbances are considered constant in the prediction horizon, which makes a nonlinear programming problem become a quadratic programming problem. The external disturbances consist of high order polynomials as in [17]. Different from the proof in [19], the convergence of the proposed ESO is proved when the disturbances keep variable. A numerical example is conducted to prove the advancement of the proposed method compared with the previous method in [19], and the proposed method is applied for the vessel heading control in presence of disturbances and unknown states in comparison with PID (proportional-integral-derivative) method.

The remainder of this article is organized as follows. Generalized ESO is introduced in Section 2. In Section 3, an improved ESO based on the generalized ESO, i.e., state-compensation ESO (SCESO), is proposed with continuous-time and discrete-time forms. In Section 4 and 5, an SCESO based MPC scheme is elaborated on and relevant stability is analyzed. Then, a numerical example and a ship heading control case are studied in Section 6. Conclusions and future research are presented in Section 7.

## 2. Generalized extended state observer

An $n^{\text{th}}$ order SISO (single-input-single-output) standard uncertain integral chain system for a standard ESO design is denoted as follows [10,14]:

$$\begin{cases} \dot{x}_1 = x_2 \\ \dot{x}_2 = x_3 \\ \quad \vdots \\ \dot{x}_n = f_d(x_1, \dots, x_n, d(t), t) + bu \\ y = x_1, \end{cases} \tag{1}$$

where $x_1, \dots, x_n$ are the states, $u$ is the control input, $d(t)$ is the external disturbance, $y$ is the output, $b$ is the system parameter, and $f_d(x_1, \dots, x_n, d(t), t)$ is the lumped disturbances containing external disturbances and sources of mismatch between the linear model and the real nonlinear system dynamics.

However, a different system, for instance second-order system (2), is not consistent with the standard integral chain form as (1), and the channel of lumped disturbances is also different from the channel of input in system (2) [19].

$$\begin{cases} \dot{x}_1 = x_1 - 2x_2 + f(x_1, x_2, d(t), t) \\ \dot{x}_2 = x_1 + x_2 + u \end{cases} \tag{2}$$

Considering that systems not satisfying standard ESO systems, like system (2), can not be dealt with by normal ESO methods, a new system form for a generalized ESO is proposed in [19]:

$$\begin{cases} \dot{\boldsymbol{x}} = \boldsymbol{A}\boldsymbol{x} + \boldsymbol{B}u + \boldsymbol{D}f_d(\boldsymbol{x}, d(t), t) \\ y = \boldsymbol{C}\boldsymbol{x}, \end{cases} \tag{3}$$

where $\boldsymbol{x} \in \mathbb{R}^{n\times 1}$ is the state vector, $u \in \mathbb{R}$ is the control input, $y \in \mathbb{R}$ is the output and $f_d(\boldsymbol{x}, d(t), t) \in \mathbb{R}$ is the lumped disturbances. $\boldsymbol{A} \in \mathbb{R}^{n\times n}$, $\boldsymbol{B} \in \mathbb{R}^{n\times 1}$, $\boldsymbol{C} \in \mathbb{R}^{1\times n}$ and $\boldsymbol{D} \in \mathbb{R}^{n\times 1}$ are state matrix, input matrix, output matrix and disturbance matrix, respectively.

In order to estimate the states and disturbances for system (3) at the same time, the generalized ESO is utilized.

Define an extended state $x_{n+1} = f_d(\boldsymbol{x}, d(t), t)$, then system (3) is rewritten as:

$$\begin{cases} \dot{\bar{\boldsymbol{x}}} = \bar{\boldsymbol{A}}\bar{\boldsymbol{x}} + \bar{\boldsymbol{B}}u + \boldsymbol{E}h(t) \\ y = \bar{\boldsymbol{C}}\bar{\boldsymbol{x}}, \end{cases} \tag{4}$$

where $\bar{\boldsymbol{x}} = [x_1, \dots, x_{n+1}]^{\mathrm{T}}$, $h(t)$ is the derivative of $x_{n+1}$, i.e., $h(t) = \dot{x}_{n+1}$. The system matrices $\bar{\boldsymbol{A}}$, $\bar{\boldsymbol{B}}$, $\bar{\boldsymbol{C}}$ and $\boldsymbol{E}$ are denoted as follows:

$$\bar{\boldsymbol{A}} = \begin{bmatrix} \boldsymbol{A}_{n\times n}\boldsymbol{D}_{n\times 1} \\ \boldsymbol{0}_{n\times n}0_{1\times 1} \end{bmatrix}, \bar{\boldsymbol{B}} = \begin{bmatrix} \boldsymbol{B}_{n\times 1} \\ 0_{1\times 1} \end{bmatrix},$$

$$\bar{\boldsymbol{C}} = [\boldsymbol{C}_{1\times n}, 0_{1\times 1}], \boldsymbol{E} = \begin{bmatrix} \boldsymbol{0}_{n\times 1} \\ 1_{1\times 1} \end{bmatrix}.$$

For system (4), the generalized ESO is designed as follows:

$$\begin{cases} \dot{\hat{\bar{\boldsymbol{x}}}} = \bar{\boldsymbol{A}}\hat{\bar{\boldsymbol{x}}} + \bar{\boldsymbol{B}}u + \boldsymbol{L}(y - \hat{y}) \\ \hat{y} = \bar{\boldsymbol{C}}\hat{\bar{\boldsymbol{x}}}, \end{cases} \tag{5}$$

where $\hat{\bar{\boldsymbol{x}}} = [\hat{x}_1, \dots, \hat{x}_{n+1}]^{\mathrm{T}}$ is the estimation of $\bar{\boldsymbol{x}}$, and $\boldsymbol{L}$ is the observer gain with dimension $n+1$ to be designed.

Define the observer estimation errors, or observer errors, as $\boldsymbol{e} = \bar{\boldsymbol{x}} - \hat{\bar{\boldsymbol{x}}}$. Combining (4) and (5), the observer errors $\boldsymbol{e}$ are given by:

$$\dot{\boldsymbol{e}} = \boldsymbol{A}_e\boldsymbol{e} + \boldsymbol{E}h(t), \tag{6}$$

where $\boldsymbol{A}_e = \bar{\boldsymbol{A}} - \boldsymbol{L}\bar{\boldsymbol{C}}$.

The bounded stability of the generalized ESO is summarized in the following lemma.

**Lemma 1** [10]**.** *Assuming that $\boldsymbol{A}_e$ is a Hurwitz matrix with a suitable $\boldsymbol{L}$ and lumped disturbances $f_d(\boldsymbol{x}, d(t), t)$ are differentiable on $t$, then the observer errors $\boldsymbol{e}$ are bounded for any bounded $h(t)$. Moreover, the boundary of $\boldsymbol{e}$ satisfies $\|\boldsymbol{e}\|_2 = 2\|\boldsymbol{P}h(t)\|_2$, where $\boldsymbol{P}$ is the unique solution of the Lyapunov equation $\boldsymbol{A}_e^{\mathrm{T}}\boldsymbol{P} + \boldsymbol{P}\boldsymbol{A}_e = -\boldsymbol{I}$ with $\boldsymbol{I}$ being an identity matrix.*

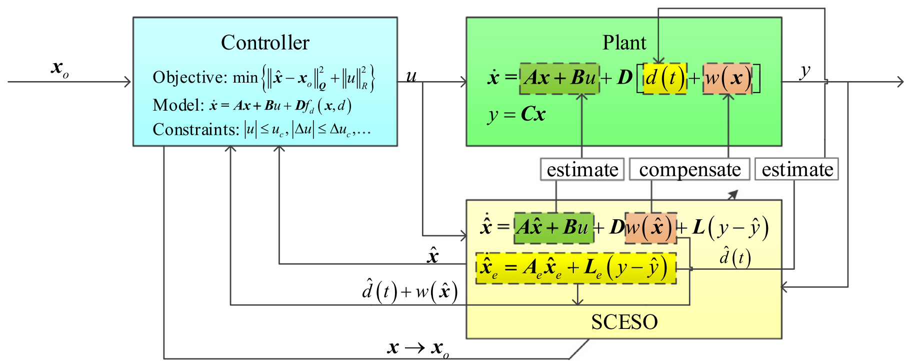


**Fig. 1.** The SCESO schema.

However, to guarantee the observer errors $\boldsymbol{e}\to\boldsymbol{0}$ when $t\to\infty$, assumptions must be satisfied using the composite control strategy [19]. The lemma for guaranteeing $\boldsymbol{e}\to\boldsymbol{0}$ when $t\to\infty$ is as follows:

**Lemma 2** [19]**.** *Suppose that $f_d(\boldsymbol{x}, d(t), t)$ equaling $f(d(t), t)$, is bounded, differentiable on $t$, and has a constant value at the steady state, which means $\lim_{t\to\infty}\dot{f}(d(t),t)=0$ and $\lim_{t\to\infty}f(d(t),t)=c$ where $c$ is a constant. Then $\boldsymbol{e}\to\boldsymbol{0}$ and $y\to 0$ when $t\to\infty$ are guaranteed if $\boldsymbol{A}_e$ and $\boldsymbol{A}_m=\boldsymbol{A}+\boldsymbol{B}\boldsymbol{K}_x$ are Hurwitz matrices and $\boldsymbol{C}\boldsymbol{A}_m^{-1}\boldsymbol{B}$ is invertible with the composite control law as $u=\boldsymbol{K}_x\hat{\boldsymbol{x}}+K_d\hat{x}_{n+1}$, where $\boldsymbol{K}_x$ is the feedback control gain and $K_d$ is the disturbance compensation gain.*

## 3. State-compensation extended state observer

For Lemma 2, the assumptions are not always satisfied if the lumped disturbances contain a nonlinear term $w(\boldsymbol{x})$, i.e., $f_d(\boldsymbol{x}, d(t), t)\neq f(d(t), t)$, or if lumped disturbances are not constant at the steady state, or if there exist constraints on system inputs. To handle systems where the assumptions for Lemma 2 are not satisfied, in this section, an improved generalized ESO, i.e., state-compensation extend state observer (SCESO), is proposed. A continuous-time SCESO is developed firstly, then a discrete-time SCESO is proposed by the zero-order hold (ZOH).

### *3.1. Continuous-time observer*

It is assumed that $f_d(\boldsymbol{x},d(t),t)=w(\boldsymbol{x})+d(t)$. For the nonlinear term $w(\boldsymbol{x})$, the function express $y_n=w(\boldsymbol{x})$ is known, but the value of $w(\boldsymbol{x})$ is unknown because $\boldsymbol{x}$ cannot be obtained directly. The external disturbances $d(t)$ are supposed to be with higher order [17], which are given by:

$$d(t)=\sum_{i=0}^{q}d_it^i, \tag{7}$$

where $q$ is the order of $d(t)$, $d_i$ is the system parameter.

Based on Lemma 1, the bounded stability of $\boldsymbol{e}$ can be obtained if there are Hurwitz matrix $\boldsymbol{A}_e$ and bounded $h(t)$. To attenuate the observer errors $\boldsymbol{e}$, $f_d(\boldsymbol{x}, d(t), t)$ should be estimated accurately. Considering that $d^{(q+1)}(t)=0$ and $w(\boldsymbol{x})$ can be estimated by updated state estimation $\hat{\boldsymbol{x}}$, an observer is designed to deal with $w(\boldsymbol{x})$ and $d(t)$ separately. That is, $w(\boldsymbol{x})$ is compensated by $w(\hat{\boldsymbol{x}})$ as in [8], and $d(t)$ is attenuated with extended states. The schema of the SCESO is shown in Fig. 1. In Fig. 1, $\boldsymbol{x}_e=[x_{n+1},\ldots,x_{n+q+1}]^{\mathrm{T}}$ is the extended state vector, and $\boldsymbol{L}\in\mathbb{R}^{n\times 1}$ and $\boldsymbol{L}_e\in\mathbb{R}^{(q+1)\times 1}$ are observer gains. The objective of the controller is to achieve $\boldsymbol{x}\to\boldsymbol{x}_o$ with the least energy consumption considering the constraints, where $\boldsymbol{x}_o$ is the objective and stable states. The SCESO is to provide the information of states and disturbances for the controller.

For system (3), the SCESO is designed as follows:

$$\begin{cases}\dot{\hat{\boldsymbol{x}}}_f=\boldsymbol{A}_f\hat{\boldsymbol{x}}_f+\boldsymbol{B}_fu+\boldsymbol{D}_f\bar{w}(\hat{\boldsymbol{x}}_f)+\boldsymbol{L}_f(y-\hat{y})\\ \hat{y}=\boldsymbol{C}_f\hat{\boldsymbol{x}}_f,\end{cases} \tag{8}$$

where the new states are redefined as $\boldsymbol{x}_f=[\boldsymbol{x}^{\mathrm{T}},\boldsymbol{x}_e^{\mathrm{T}}]^{\mathrm{T}}$, $\bar{w}(\hat{\boldsymbol{x}}_f)=w(\hat{\boldsymbol{x}})$, and $x_{n+1}=d(t)$, $x_{n+2}=\dot{d}(t)$, $\ldots$, $x_{n+q+1}=d^{(q)}(t)$. The SCESO matrices are shown as follows:

$$\boldsymbol{A}_f=\begin{bmatrix}\boldsymbol{A}_{n\times n}&\boldsymbol{D}_{n\times 1}&\boldsymbol{0}_{n\times q}\\ \boldsymbol{0}_{q\times n}&\boldsymbol{0}_{q\times 1}&\boldsymbol{I}_{q\times q}\\ \boldsymbol{0}_{1\times n}&0_{1\times 1}&\boldsymbol{0}_{1\times q}\end{bmatrix},\boldsymbol{B}_f=\begin{bmatrix}\boldsymbol{B}\\ \boldsymbol{0}_{(q+1)\times 1}\end{bmatrix},$$

$$\boldsymbol{C}_f=\begin{bmatrix}\boldsymbol{C}_{1\times n}&\boldsymbol{0}_{1\times(q+1)}\end{bmatrix},\boldsymbol{D}_f=\begin{bmatrix}\boldsymbol{D}_{n\times 1}\\ \boldsymbol{0}_{(q+1)\times 1}\end{bmatrix}.$$

The observer gain $\boldsymbol{L}_f=[\boldsymbol{L}^{\mathrm{T}},\boldsymbol{L}_e^{\mathrm{T}}]^{\mathrm{T}}=[\beta_1,\ldots,\beta_{n+q+1}]^{\mathrm{T}}$.

Then system (3) can be transformed as follows:

$$\begin{cases}\dot{\boldsymbol{x}}_f=\boldsymbol{A}_f\boldsymbol{x}_f+\boldsymbol{B}_fu+\boldsymbol{D}_f\bar{w}(\boldsymbol{x}_f)\\ y=\boldsymbol{C}_f\boldsymbol{x}_f.\end{cases} \tag{9}$$

The observer errors $\boldsymbol{e}_f=\boldsymbol{x}_f-\hat{\boldsymbol{x}}_f$ are obtained based on (9) and (8), which are given by:

$$\dot{\boldsymbol{e}}_f=(\boldsymbol{A}_f-\boldsymbol{L}_f\boldsymbol{C}_f)\boldsymbol{e}_f+\boldsymbol{D}_f(\bar{w}(\boldsymbol{x}_f)-\bar{w}(\hat{\boldsymbol{x}}_f)) \tag{10}$$

**Remark 1.** Assuming that $\|\bar{w}(\boldsymbol{x}_f)\|_2$ and $\|\bar{w}(\hat{\boldsymbol{x}}_f)\|_2$ are bounded, then $\|\bar{w}(\boldsymbol{x}_f)-\bar{w}(\hat{\boldsymbol{x}}_f)\|_2\leqslant\|\bar{w}(\boldsymbol{x}_f)\|_2+\|\bar{w}(\hat{\boldsymbol{x}}_f)\|_2$ is also bounded. Therefore, with Lemma 1, it is obtained that $\boldsymbol{e}_f\le\boldsymbol{e}_0$ is bounded where $\boldsymbol{e}_0$ is a positive constant if $(\boldsymbol{A}_f-\boldsymbol{L}_f\boldsymbol{C}_f)$ is a Hurwitz matrix.

**Lemma 3** [44]**.** *Define that $Co(\boldsymbol{a},\boldsymbol{b})=\{\lambda\boldsymbol{a}+(1-\lambda)\boldsymbol{b}, 0\leqslant\lambda\leqslant 1\}$ is the convex hull of $\{\boldsymbol{a}, \boldsymbol{b}\}$. Assuming that $\bar{w}(\boldsymbol{X})$ is differentiable on $Co(\boldsymbol{x}_f,\hat{\boldsymbol{x}}_f)$, where $\boldsymbol{X}$ has the same dimension as $\boldsymbol{x}_f$ and $\hat{\boldsymbol{x}}_f$, then there exists a constant vector $\boldsymbol{z}\in Co(\boldsymbol{x}_f,\hat{\boldsymbol{x}}_f)$, $\boldsymbol{z}\neq\boldsymbol{x}_f$, $\boldsymbol{z}\neq\hat{\boldsymbol{x}}_f$, such that:*

$$\bar{w}(\boldsymbol{x}_f)-\bar{w}(\hat{\boldsymbol{x}}_f)=\boldsymbol{H}(\boldsymbol{z})\boldsymbol{e}_f, \tag{11}$$

*where* $\boldsymbol{H}(\boldsymbol{z})=[\frac{\partial\bar{w}(\boldsymbol{X})}{\partial X_1},\ldots,\frac{\partial\bar{w}(\boldsymbol{X})}{\partial X_i},\ldots,\frac{\partial\bar{w}(\boldsymbol{X})}{\partial X_{n+q+1}}]|_{\boldsymbol{X}=\boldsymbol{z}}$, $\boldsymbol{X}=[X_1,X_2,\ldots,X_{n+q+1}]^{\mathrm{T}}$.

Combining (10) and Lemma 3, it is obtained that:

$$\dot{\boldsymbol{e}}_f=[\boldsymbol{A}_f-\boldsymbol{L}_f\boldsymbol{C}_f+\boldsymbol{D}_f\boldsymbol{H}(\boldsymbol{z})]\boldsymbol{e}_f. \tag{12}$$

To realize $\boldsymbol{e}_f\to\boldsymbol{0}$ when $t\to\infty$, one solution is to design a constant Hurwitz matrix $[\boldsymbol{A}_f-\boldsymbol{L}_f\boldsymbol{C}_f+\boldsymbol{D}_f\boldsymbol{H}(\boldsymbol{z})]$. Considering that MPC method can optimize a cost function such that $\hat{\boldsymbol{x}}$ converges to an equilibrium point and has advantages of dealing with system constraints [22], it is reasonable to combine SCESO and MPC to realize the control objective when there exist disturbances, unmeasurable states and constraints in the system.

### 3.2. Discrete-time observer

For MPC, an online optimization problem with constraints needs to be solved by a digital computer [24]. Therefore, a continuous prediction model needs to be discretized [2,29].

A continuous-time model is usually discretized by the ZOH assumption in practice [23]. Therefore, model (3) is first discretized as:

$$\begin{cases} \boldsymbol{x}(k+1) = \boldsymbol{A}_c\boldsymbol{x}(k) + \boldsymbol{B}_c u(k) + \boldsymbol{D}_c f_d(\boldsymbol{x}(k), d(k), T_s) \\ y(k) = \boldsymbol{C}_c\boldsymbol{x}(k), \end{cases} \tag{13}$$

where $T_s$ is the sampling time and $k$ is a discrete time step standing for time instant $kT_s$. $\boldsymbol{A}_c$, $\boldsymbol{B}_c$, $\boldsymbol{C}_c$ and $\boldsymbol{D}_c$ are discrete-time system matrices.

SCESO (8) is also discretized with ZOH as follows:

$$\begin{cases} \hat{\boldsymbol{x}}_f(k+1) = \boldsymbol{A}_{fc}\hat{\boldsymbol{x}}_f(k) + \boldsymbol{B}_{fc}u(k) + \boldsymbol{D}_{fc}\bar{w}(\hat{\boldsymbol{x}}_f(k)) \\ \qquad\qquad\qquad + \boldsymbol{L}_{fc}(y(k) - \hat{y}(k)) \\ \hat{y}(k) = \boldsymbol{C}_{fc}\hat{\boldsymbol{x}}_f(k), \end{cases} \tag{14}$$

where $\boldsymbol{L}_{fc} = [\beta_{c1}, \beta_{c2}, \ldots, \beta_{c(n+q+1)}]^{\mathrm{T}}$, $\boldsymbol{A}_{fc}$, $\boldsymbol{B}_{fc}$, $\boldsymbol{C}_{fc}$ and $\boldsymbol{D}_{fc}$ are discrete-time system matrices. Accordingly, system (9) can be transformed as follows:

$$\begin{cases} \boldsymbol{x}_f(k+1) = \boldsymbol{A}_{fc}\boldsymbol{x}_f(k) + \boldsymbol{B}_{fc}u(k) + \boldsymbol{D}_{fc}\bar{w}(\boldsymbol{x}_f(k)) \\ y(k) = \boldsymbol{C}_{fc}\boldsymbol{x}_f(k). \end{cases} \tag{15}$$

## 4. SCESO based model predictive control

MPC is used to design a controller to optimize the tracking performance considering system constraints. The prediction model is based on the nominal dynamics that are updated by the SCESO observer (8). Without loss of generality, the control objective is to achieve $\boldsymbol{x} \to \boldsymbol{x}_o$ where $\boldsymbol{x}_o$ is the objective and stable state vector. Therefore, the cost function $J(k)$ at instant time $k$ is defined as follows:

$$J(k) = \sum_{i=1}^{N_P} \left\{ \|\tilde{\boldsymbol{x}}(k+i) - \boldsymbol{x}_o\|_{\boldsymbol{Q}}^2 + \|\tilde{u}(k+i-1)\|_R^2 \right\}, \tag{16}$$

where $\boldsymbol{Q} \geq 0$ and $R > 0$ are the weighting matrix and parameter, respectively, and $N_P$ is the length of the prediction horizon. $\tilde{\boldsymbol{x}}(k+i)$ and $\tilde{u}(k+i-1)$ are predictive system states at time $k+i$ and input at time time $k+i-1$, respectively.

The optimization problem is to minimize the cost function $J(k)$ online subject to system constraints as follows:

$$\tilde{\boldsymbol{u}}^*(k) = \underset{\tilde{\boldsymbol{u}}(k)}{\operatorname{argmin}}\, J(k), \tag{17}$$

subject to

$$\begin{aligned} &\tilde{\boldsymbol{x}}(k+i) = \boldsymbol{A}_c\tilde{\boldsymbol{x}}(k+i-1) + \boldsymbol{B}_c\tilde{u}(k+i-1) \\ &\qquad\qquad + \boldsymbol{D}_c f_d(\hat{\boldsymbol{x}}(k), \hat{d}(k), T_s) \\ &f_d(\hat{\boldsymbol{x}}(k), \hat{d}(k), T_s) = w(\hat{\boldsymbol{x}}(k)) + \hat{d}(k) \\ &\hat{d}(k) = \hat{x}_{n+1}(k),\ \tilde{\boldsymbol{x}}(k) = \hat{\boldsymbol{x}}(k),\ \tilde{u}(k-1) = u(k-1) \\ &\hat{\boldsymbol{x}}_f(k) = [\hat{\boldsymbol{x}}(k)^{\mathrm{T}}, \hat{x}_{n+1}(k), \ldots, \hat{x}_{n+q+1}(k)]^{\mathrm{T}} \\ &\boldsymbol{x}_{\min} \leqslant \tilde{\boldsymbol{x}}(k+i) \leqslant \boldsymbol{x}_{\max} \\ &u_{\min} \leqslant \tilde{u}(k+i-1) \leqslant u_{\max} \\ &\Delta u_{\min} \leqslant \Delta\tilde{u}(k+i-1) \leqslant \Delta u_{\max} \\ &\Delta\tilde{u}(k+i-1) = \tilde{u}(k+i-1) - \tilde{u}(k+i-2) \\ &i = 1, 2, \ldots, N_P, \end{aligned}$$

where $\tilde{\boldsymbol{u}}^*(k) = [\tilde{u}^*(k), \ldots, \tilde{u}^*(k+N_{\mathrm{P}}-1)]^{\mathrm{T}}$ is the optimal input sequence. $\tilde{\boldsymbol{u}}(k) = [\tilde{u}(k), \ldots, \tilde{u}(k+N_{\mathrm{P}}-1)]^{\mathrm{T}}$ is the independent argument of $J(k)$, $\hat{\boldsymbol{x}}_f(k)$ is estimated by the proposed SCESO (14), $u(k-1)$ is measured at time $k-1$, $\boldsymbol{x}_{\min}$ and $\boldsymbol{x}_{\max}$ are system state constraints, and $u_{\min}$, $u_{\max}$, $\Delta u_{\min}$ and $\Delta u_{\max}$ are system input constraints.

Based on MPC and the proposed observer strategy, a proposed observer based control algorithm is summarized in Algorithm 1.

**Algorithm 1** Proposed observer based control algorithm.

1: Set $k = 0$, and initialize system states $\hat{\boldsymbol{x}}_f(0)$ and input $u(0)$;
2: **while** The control process is not ended **do**
3: Solve problem (17) online with known $\hat{\boldsymbol{x}}_f(k)$ to obtain the optimal input sequence $\tilde{\boldsymbol{u}}^*(k)$;
4: Apply the first element of $\tilde{\boldsymbol{u}}^*(k)$, i.e., $\tilde{u}^*(k)$, to system dynamics;
5: Measure the current state $y(k+1)$ at the time $k+1$;
6: Estimate $\hat{\boldsymbol{x}}_f(k+1)$ based on $u(k)$, $\hat{\boldsymbol{x}}_f(k)$ and $y(k+1)$ by the proposed SCESO (14);
7: $k = k+1$.
8: **end while**

## 5. Stability analysis for observer

**Assumption 1.** a) The order of external disturbances in (7), i.e., $q$, is known; b) $f_d(\boldsymbol{x}, d(t), t)$ is differentiable on $t$; c) $\|\bar{w}(\boldsymbol{x}_f)(k)\|_2$ and $\|\bar{w}(\hat{\boldsymbol{x}}_f)(k)\|_2$ are bounded.

**Assumption 2.** The $i^{\mathrm{th}}$ eigenvalue $\lambda_i\,(i = 1, \ldots, n+q+1)$ of $\boldsymbol{A}_{fc}^e$ satisfies $|\lambda_i| < 1$ where $\boldsymbol{A}_{fc}^e = \boldsymbol{A}_{fc} - \boldsymbol{L}_{fc}\boldsymbol{C}_{fc}$.

**Theorem 1.** *If the Assumptions 1 and 2 are satisfied, the observer error $\boldsymbol{e}_f(k)$ of SCESO is bounded, where $\boldsymbol{e}_f(k) = \boldsymbol{x}_f(k) - \hat{\boldsymbol{x}}_f(k)$.*

**Proof.** Based on (15) and (14), $\boldsymbol{e}_f$ is obtained:

$$\boldsymbol{e}_f(k+1) = \boldsymbol{A}_{fc}^e\boldsymbol{e}_f(k) + \Delta\bar{\boldsymbol{w}}(k), \tag{18}$$

where $\Delta\bar{\boldsymbol{w}}(k) = \boldsymbol{D}_{fc}[\bar{w}(\boldsymbol{x}_f(k)) - \bar{w}(\hat{\boldsymbol{x}}_f(k))]$. With $|\lambda_i| < 1$, let a Lyapunov function set as $V(\boldsymbol{e}_f(k)) = \boldsymbol{e}_f(k)^{\mathrm{T}}\boldsymbol{P}\boldsymbol{e}_f(k)$, where $\boldsymbol{P}$ is the unique solution of Lyapunov equation $[\boldsymbol{A}_{fc}^e]^{\mathrm{T}}\boldsymbol{P}\boldsymbol{A}_{fc}^e - \boldsymbol{P} = -\boldsymbol{Q}$, $\boldsymbol{P} > 0$ and $\boldsymbol{Q} > 0$ are both symmetric matrices [16]. Combining (15), then

$$\begin{aligned} \Delta V(\boldsymbol{e}_f(k)) &= V(\boldsymbol{e}_f(k)) - V(\boldsymbol{e}_f(k-1)) \\ &= -[\boldsymbol{e}_f(k-1)]^{\mathrm{T}}\boldsymbol{Q}\boldsymbol{e}_f(k-1) \\ &\quad + 2[\Delta\bar{\boldsymbol{w}}(k-1)]^{\mathrm{T}}\boldsymbol{P}\boldsymbol{A}_{fc}^e\boldsymbol{e}_f(k-1) \\ &\quad + [\Delta\bar{\boldsymbol{w}}(k-1)]^{\mathrm{T}}\boldsymbol{P}\Delta\bar{\boldsymbol{w}}(k-1) \\ &= -\|\boldsymbol{M}(k-1) - \boldsymbol{N}(k-1)\|_2^2 \\ &\quad + \|\boldsymbol{N}(k-1)\|_2^2 + \|\boldsymbol{W}(k-1)\|_2^2, \end{aligned} \tag{19}$$

where $\boldsymbol{M}(k-1) = [\boldsymbol{e}_f(k-1)]^{\mathrm{T}}\boldsymbol{Q}^{\frac{1}{2}}$, $\boldsymbol{N}(k-1) = [\Delta\bar{\boldsymbol{w}}(k-1)]^{\mathrm{T}}\boldsymbol{P}\boldsymbol{A}_{fc}^e\boldsymbol{Q}^{-\frac{1}{2}}$ and $\boldsymbol{W}(k-1) = [\Delta\bar{\boldsymbol{w}}(k-1)]^{\mathrm{T}}\boldsymbol{P}^{\frac{1}{2}}$.

From Assumption 1, $\|\bar{w}(\boldsymbol{x}_f)(k)\|_2$ and $\|\bar{w}(\hat{\boldsymbol{x}}_f)(k)\|_2$ are bounded, then $\|\Delta\bar{\boldsymbol{w}}(k-1)\|_2 \leqslant \|\boldsymbol{D}_{fc}\|_2(\|\bar{w}(\boldsymbol{x}_f)(k)\|_2 + \|\bar{w}(\hat{\boldsymbol{x}}_f)(k)\|_2)$ is also bounded. Therefore, $\|\boldsymbol{N}(k-1)\|_2^2 + \|\boldsymbol{W}(k-1)\|_2^2$ is bounded since:

$$\begin{aligned} &\|\boldsymbol{N}(k-1)\|_2^2 + \|\boldsymbol{W}(k-1)\|_2^2 \\ &\leqslant \|\boldsymbol{P}\boldsymbol{Q}^{-\frac{1}{2}}\|_2^2\|\Delta\bar{\boldsymbol{w}}(k-1)\|_2^2 + \|\boldsymbol{P}^{\frac{1}{2}}\|_2^2\|\Delta\bar{\boldsymbol{w}}(k-1)\|_2^2 \\ &\leqslant (\|\boldsymbol{P}\boldsymbol{Q}^{-\frac{1}{2}}\|_2^2 + \|\boldsymbol{P}^{\frac{1}{2}}\|_2^2)\|\boldsymbol{D}_{fc}\|_2^2\left(\|\bar{w}(\boldsymbol{x}_f)(k)\|_2 + \left\|\bar{w}(\hat{\boldsymbol{x}}_f)(k)\right\|_2\right)^2. \end{aligned}$$

To make $\Delta V(\boldsymbol{e}_f(k)) < 0$, it should be satisfied with (19) that:

$$\|\boldsymbol{M}(k-1) - \boldsymbol{N}(k-1)\|_2^2 > \|\boldsymbol{N}(k-1)\|_2^2 + \|\boldsymbol{W}(k-1)\|_2^2. \tag{20}$$

Considering that:

$$\|\boldsymbol{M}(k-1)-\boldsymbol{N}(k-1)\|_2 \geqslant \|\boldsymbol{M}(k-1)\|_2-\|\boldsymbol{N}(k-1)\|_2,$$

if:

$$\|\boldsymbol{M}(k-1)\|_2 > \|\boldsymbol{N}(k-1)\|_2+(\|\boldsymbol{N}(k-1)\|_2^2+\|\boldsymbol{W}(k-1)\|_2^2)^{\frac{1}{2}}, \tag{21}$$

then (20) is satisfied.

For $\boldsymbol{Q}=\boldsymbol{I}$, $\Delta V(\boldsymbol{e}_f(k))<0$ if

$$\|\boldsymbol{e}_f(k-1)\|_2 > \|[\Delta\bar{\boldsymbol{w}}(k-1)]^{\mathrm{T}}\boldsymbol{P}\boldsymbol{A}_{fc}^e\|_2 + \{\|[\Delta\bar{\boldsymbol{w}}(k-1)]^{\mathrm{T}}\boldsymbol{P}\boldsymbol{A}_{fc}^e\|_2^2+\|[\Delta\bar{\boldsymbol{w}}(k-1)]^{\mathrm{T}}\boldsymbol{P}^{\frac{1}{2}}\|_2^2\}^{\frac{1}{2}}. \tag{22}$$

It can be obtained that $\|\boldsymbol{e}_f(k-1)\|_2$ decreases since $\Delta V(\boldsymbol{e}_f(k))<0$ for $\|\boldsymbol{e}_f(k-1)\|_2$ that satisfies (22). Hence $\boldsymbol{e}_f(k)$ is bounded. □

Derived from Lemma 3, a lemma for the discrete-time system is as follows:

**Lemma 4** [44]. *Assuming that $\bar{w}(\boldsymbol{X})$ is differentiable on $Co(\boldsymbol{x}_f(k),\hat{\boldsymbol{x}}_f(k))$, where $\boldsymbol{X}$ has the same dimension as $\boldsymbol{x}_f$ and $\hat{\boldsymbol{x}}_f$, then there exists a constant vector $\boldsymbol{z}(k)\in Co(\boldsymbol{x}_f(k),\hat{\boldsymbol{x}}_f(k))$, $\boldsymbol{z}(k)\neq \boldsymbol{x}_f(k)$, $\boldsymbol{z}(k)\neq\hat{\boldsymbol{x}}_f(k)$, such that:*

$$\bar{w}(\boldsymbol{x}_f(k))-\bar{w}(\hat{\boldsymbol{x}}_f(k))=\boldsymbol{H}(\boldsymbol{z})\boldsymbol{e}_f(k), \tag{23}$$

*where* $\boldsymbol{H}(\boldsymbol{z}(k))=[\frac{\partial\bar{w}(\boldsymbol{X})}{\partial X_1},\dots,\frac{\partial\bar{w}(\boldsymbol{X})}{\partial X_i},\dots,\frac{\partial\bar{w}(\boldsymbol{X})}{\partial X_{n+q+1}}]|_{\boldsymbol{X}=\boldsymbol{z}(k)}$, $\boldsymbol{X}=[X_1,X_2,\dots,X_{n+q+1}]^{\mathrm{T}}$.

**Assumption 3.** a) The estimation $\hat{\boldsymbol{x}}$ satisfies that $\lim_{k\to\infty}\hat{\boldsymbol{x}}(k)\to\boldsymbol{x}_o$ and $\lim_{k\to\infty}\boldsymbol{x}(k)\to\boldsymbol{x}_s$ with Algorithm 1, where $\boldsymbol{x}_o$ and $\boldsymbol{x}_s$ are both constant vectors; b) the $i^{\text{th}}$ eigenvalue $\lambda_i^g\,(i=1,\dots,n+q+1)$ of $\boldsymbol{A}_{fc}^g$ satisfies $|\lambda_i^g|<1$ where $\boldsymbol{A}_{fc}^g=\boldsymbol{A}_{fc}^e+\boldsymbol{D}_{fc}\boldsymbol{H}(\boldsymbol{z}(k-1))$ when $k\to\infty$.

**Remark 2.** According to Theorem 1, $\boldsymbol{e}_f(k)=\boldsymbol{x}_f(k)-\hat{\boldsymbol{x}}_f(k)$ is bounded. It also means that $\boldsymbol{e}(k)=\boldsymbol{x}(k)-\hat{\boldsymbol{x}}(k)$ is bounded. Meanwhile, when $\lim_{k\to\infty}\hat{\boldsymbol{x}}(k)\to\boldsymbol{x}_o$, $\boldsymbol{x}(k)=\boldsymbol{e}(k)+\boldsymbol{x}_o$ is bounded. Therefore, it is reasonable to assume that $\boldsymbol{z}(k)\in Co(\boldsymbol{x}_f(k),\hat{\boldsymbol{x}}_f(k))$ is a neighborhood of $[\boldsymbol{x}_o^{\mathrm{T}},\boldsymbol{0}^{\mathrm{T}}]^{\mathrm{T}}$, such that $\boldsymbol{L}_{fc}$ can be designed to make the $i^{\text{th}}$ eigenvalue $\lambda_i^g\,(i=1,\dots,n+q+1)$ of $\boldsymbol{A}_{fc}^g$ satisfy $|\lambda_i^g|<1$.

**Theorem 2.** *Suppose that Assumptions 1, 2 and–3 are satisfied, then the observer errors $\lim_{k\to\infty}\boldsymbol{e}_f(k)\to\boldsymbol{0}$ and the system states $\lim_{k\to\infty}\boldsymbol{x}(k)\to\boldsymbol{x}_o$.*

**Proof.** Combining (18) and Lemma 4, $\boldsymbol{e}_f(k)$ is denoted as follows:

$$\boldsymbol{e}_f(k)=[\boldsymbol{A}_{fc}^e+\boldsymbol{D}_{fc}\boldsymbol{H}(\boldsymbol{z}(k-1))]\boldsymbol{e}_f(k-1). \tag{24}$$

According to Assumption 3, when $k\to\infty$, $\lim_{k\to\infty}\hat{\boldsymbol{x}}(k)\to\boldsymbol{x}_o$ and $\lim_{k\to\infty}\boldsymbol{x}(k)\to\boldsymbol{x}_s$.

Define $\boldsymbol{H}_1=[\frac{\partial w(\boldsymbol{x})}{\partial x_1},\dots,\frac{\partial w(\boldsymbol{x})}{\partial x_i},\dots,\frac{\partial w(\boldsymbol{x})}{\partial x_n}]|_{\boldsymbol{x}=\boldsymbol{z}_1(k-1)}$ with $\boldsymbol{z}_1(k-1)\in Co(\boldsymbol{x}(k-1),\hat{\boldsymbol{x}}(k-1))$, and considering that $\bar{w}(\boldsymbol{X})=w(\boldsymbol{x})$, it is obtained that:

$$\begin{aligned}\boldsymbol{D}_{fc}\boldsymbol{H}(\boldsymbol{z}(k-1))&=\begin{bmatrix}\boldsymbol{D}_c\\ \boldsymbol{0}\end{bmatrix}\left[\frac{\partial\bar{w}(\boldsymbol{X})}{\partial X_1},\dots,\frac{\partial\bar{w}(\boldsymbol{X})}{\partial X_i},\dots,\frac{\partial\bar{w}(\boldsymbol{X})}{\partial X_{n+q+1}}\right]\Bigg|_{\boldsymbol{X}=\boldsymbol{z}(k-1)}\\ &=\begin{bmatrix}\boldsymbol{D}_c\\ \boldsymbol{0}\end{bmatrix}\left[\frac{\partial w(\boldsymbol{x})}{\partial x_1},\dots,\frac{\partial w(\boldsymbol{x})}{\partial x_i},\dots,\frac{\partial w(\boldsymbol{x})}{\partial x_n},\boldsymbol{0}_{q+1}\right]\Bigg|_{\boldsymbol{x}=\boldsymbol{z}_1(k-1)}\\ &=\begin{bmatrix}\boldsymbol{D}_c\boldsymbol{H}_1 & \boldsymbol{0}_{n\times(q+1)}\\ \boldsymbol{0}_{(q+1)\times n} & \boldsymbol{0}_{(q+1)\times(q+1)}\end{bmatrix}\end{aligned}$$

According to Assumption 3, it can be obtained that $\lim_{k\to\infty}\hat{\boldsymbol{x}}(k)\to\boldsymbol{x}_o$ and $\lim_{k\to\infty}\boldsymbol{x}(k)\to\boldsymbol{x}_s$. Based on it, $\lim_{k\to\infty}\boldsymbol{z}_1(k-1)=Co(\boldsymbol{x}_o,\boldsymbol{x}_s)$ is a constant vector, and $\lim_{k\to\infty}\boldsymbol{D}_c\boldsymbol{H}_1$ is also a constant vector. It can be deduced that $\lim_{k\to\infty}\boldsymbol{D}_{fc}\boldsymbol{H}(\boldsymbol{z}(k-1))\to\boldsymbol{A}_z$ where $\boldsymbol{A}_z$ is a constant matrix, and $\boldsymbol{A}_{fc}^g=\boldsymbol{A}_{fc}^e+\boldsymbol{A}_z$ is a constant matrix.

Considering that all eigenvalues of $\boldsymbol{A}_{fc}^g$ have magnitudes less than 1 according to Assumption 3, system (24) is asymptotically stable, i.e., $\lim_{k\to\infty}\boldsymbol{e}_f(k)\to\boldsymbol{0}$ [3]. Based on $\boldsymbol{e}_f(k)=\boldsymbol{x}_f-\hat{\boldsymbol{x}}_f$, $\lim_{k\to\infty}\boldsymbol{e}_f(k)\to\boldsymbol{0}$ and $\lim_{k\to\infty}\hat{\boldsymbol{x}}(k)\to\boldsymbol{x}_0$, it can be obtained that $\lim_{k\to\infty}\boldsymbol{x}(k)\to\boldsymbol{x}_0$, i.e., $\boldsymbol{x}_s=\boldsymbol{x}_0$. □

In summary, the observer errors of the proposed SCESO can be guaranteed to be bounded if Assumption 1 and 2 are satisfied, and the observer errors will not converge to $\boldsymbol{0}$ asymptotically unless MPC controller satisfies $\lim_{k\to\infty}\hat{\boldsymbol{x}}(k)\to\boldsymbol{x}_o$ and $\lim_{k\to\infty}\boldsymbol{x}(k)\to\boldsymbol{x}_s$.

## 6. Case study

To verify the effectiveness of the proposed SCESO approach, simulation experiments are conducted. Firstly, a numerical example in [19] is presented and the control performance with the proposed method is compared with the control performance with the method proposed in [19], then an application of the proposed control and observer strategy to ship heading control is presented.

### 6.1. Case 1: Numerical example

#### 6.1.1. Setup

A second-order uncertain nonlinear system is considered as [19]:

$$\begin{cases}\dot{x}_1=x_2+e^{x_1}+d\\ \dot{x}_2=-2x_1-x_2+u\\ y=x_1,\end{cases} \tag{25}$$

To be consistent with system (3), the system matrices are set as $\boldsymbol{A}=[\begin{smallmatrix}0&1\\-2&-1\end{smallmatrix}]$, $\boldsymbol{B}=[0,1]^{\mathrm{T}}$, $\boldsymbol{C}=[1,0]$, $\boldsymbol{D}=[1,0]^{\mathrm{T}}$ and $f_d(\boldsymbol{x},d(t),t)=e^{x_1}+d$.

The initial states of system (25) are $\boldsymbol{x}(0)=[1,0]^{\mathrm{T}}$. The external disturbance $d=3$ acts on the system at $t=6$ s. The control objective is to let the setpoint of the output $y$ be 0 while rejecting the influence of disturbances. According to Theorem 2, the observer gain is chosen as $L_{fc}=[0.30,-0.17,0.41]^{\mathrm{T}}$ such that the eigenvalues of $\boldsymbol{A}_{fc}^e$ and $\boldsymbol{A}_{fc}^g$ are $[0.94,\,0.94,\,0.77]^{\mathrm{T}}$ and $[0.90,\,0.90,\,0.90]^{\mathrm{T}}$, respectively. For the MPC controller, the objective states should be set as $[x_{1o},x_{2o}]^{\mathrm{T}}=[0,0]^{\mathrm{T}}$. The MPC parameters are set as: $N_P=20$, $\boldsymbol{Q}=\mathrm{diag}[100,0.1]$, $R=0.1$ for (16), and the sample time for discretization and control $T_s=0.05$ s. The constraint of input $u$ is limited to $[-30,30]$.

#### 6.1.2. Results

The real states, estimated states and observer errors of state $x_1$, $x_2$ and lumped disturbances $f_d(\boldsymbol{x},\,d(t),\,t)$ are shown in 2–4. The input $u$ is shown in Fig. 5. To guarantee the conformity of observer error definition with that in [19], the definition of observer errors $\boldsymbol{e}$ changes to $-\boldsymbol{e}$ named negative observer errors in Figs. 2–4,7. Note that the definition of lumped disturbances in Fig. 4 is consistent with that in [19]. From the simulation results, it is observed that all observer errors $\boldsymbol{e}$ converge to $\boldsymbol{0}$ after $t=9.0$ s in Figs. 2–4, and the output $y$ (i.e., $x_1$) can keep the objective value 0 stably with $u=-4.0$ in Fig. 5.

To be compared with the results with generalized extended state observer based control (GESOBC) in [19], the comparison of output $y$ is shown in Fig. 6. From this figure, it is obvious that system output $y$ converges to the objective value 0

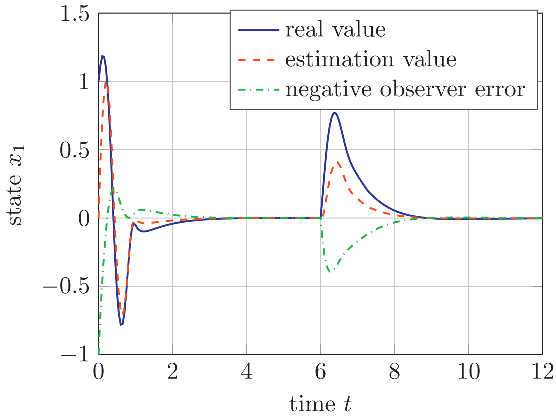


**Fig. 2.** The real and estimated values of state $x_1$.

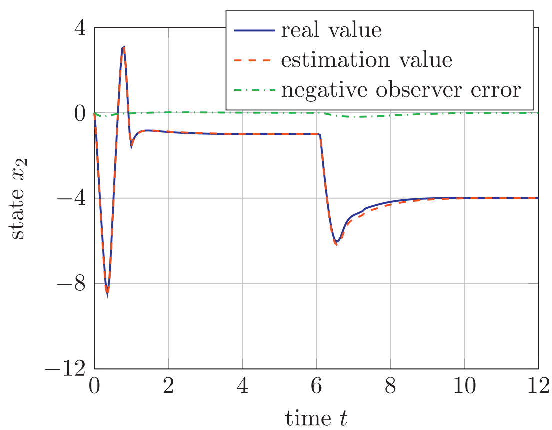


**Fig. 3.** The real and estimated values of state $x_2$.

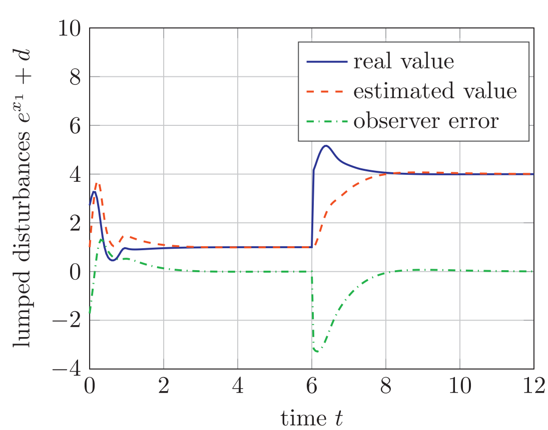


**Fig. 4.** The real and estimated values of lumped disturbances.

faster with the SCESO based MPC than with the GESOBC. The integral performance index for the integral of absolute error is usually used for evaluating the performance of a controller [34]. The *integral of absolute error* index is denoted as $\int_0^\infty |e(t)|dt$ where $e(t)$ is the tracking error until $t$. A similar index is introduced for a discrete-time system, i.e., the summation of absolute error, which is defined as $summation\ of\ absolute\ error(t_d) = \sum_{k=1}^{(1+t_d/T_s)} |e(k)|T_s$, for evaluating the control performance until $t_d$. The $summation\ of\ absolute\ error(12s) = 0.2605$ for the GESOBC. By contrast, The $summation\ of\ absolute\ error(12\,s) = 0.1192$ for the SCESO based MPC. These results also mean that the proposed

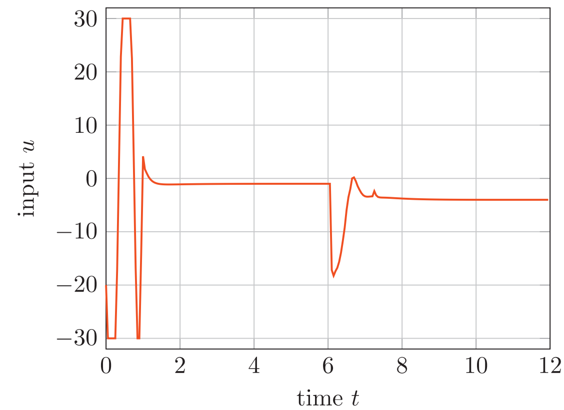


**Fig. 5.** The input $u$ values during simulation.

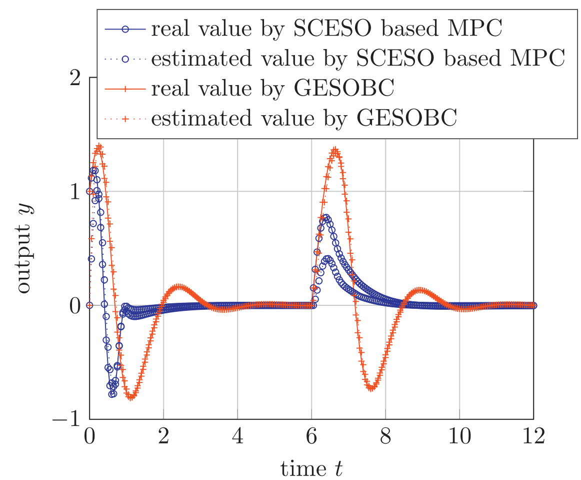


**Fig. 6.** The real and estimated values of output $y$ by SCESO based MPC and GESOBC.

SCESO based MPC method can deal with the mismatched disturbances like in system (25).

From the numerical calculation, it is found that the eigenvalues of $\boldsymbol{A}^e_{fc}$ and $\boldsymbol{A}^g_{fc}$ has an influence on the convergence of the state estimation and control performance. For the sake of simplification, it is assumed that the eigenvalue absolute array of $\boldsymbol{A}^g_{fc}$ is set as $[\lambda_a, \ldots, \lambda_a]_{1\times(n+q+1)}$ with $0 < \lambda_a < 1$. The real state and observer error of $x_1$ are shown in Fig. 7 with $\lambda_a = \{0.7, 0.8, 0.9, 0.95\}$. In general, if a larger $\lambda_a$ is used in the system, the observer error variance is smaller while the convergence speed of the state is slower. For instance, the $x_1$ observer error does not approach to 0 even after $t = 8$ s with $\lambda_a = 0.95$. In contrast, if a smaller $\lambda_a$ is used, the observer error variance is bigger, which can generate inappropriate control inputs to the system and result in poor control performance, such as when $\lambda_a = 0.70$. Taking into account these aspects, $\lambda_a = 0.90$ is selected in this simulation.

### 6.2. Case 2: Ship heading control

Autonomous vessels have received much attention recently. One challenge for autonomous vessels is to track a preplanned path with unknown states under the disturbances of current, wind and waves [1,20,25,45]. In practice, the preplanned path is usually tracked by adjusting the heading with the assumption of constant vessel speed. To this end, a nonlinear SISO model, a second-order Nomoto model, can be used as the motion control model.

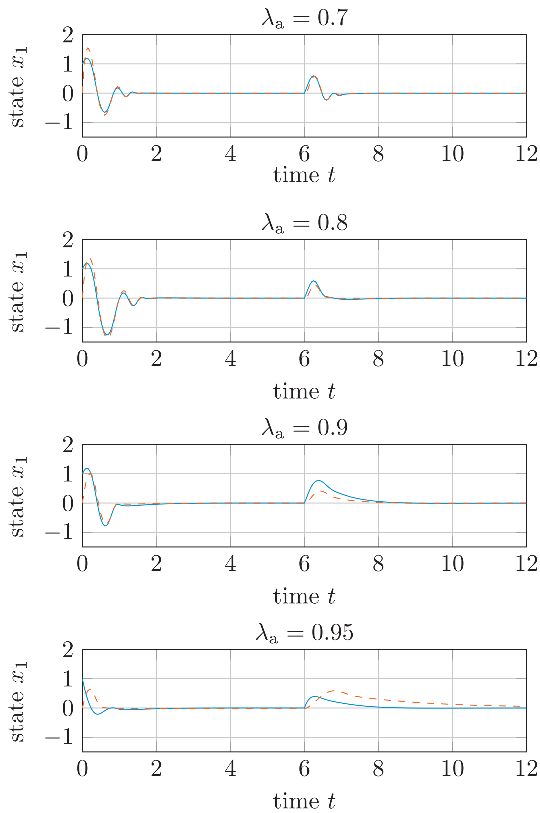


**Fig. 7.** The real value and estimation value of state $x_1$ with different $\lambda_a$ (blue solid line: real value, red dotted line: estimation value).

*6.2.1. Setup*

In this model, the state is defined as $\boldsymbol{x} = [x_1, x_2, x_3, x_4]^{\mathrm{T}}$, where $x_1$, $x_2$, $x_3$, and $x_4$ are the heading, heading rate, heading acceleration and real rudder angle, respectively. The input is the rudder order $u$. The output is the heading $y = x_1$ that can be measured by sensors directly. The state-space equations of second-order Nomoto model are shown as follows:

$$\begin{cases} \dot{x}_1 = x_2 \\ \dot{x}_2 = x_3 \\ \dot{x}_3 = g(\boldsymbol{x}, u) + d(t) \\ \dot{x}_4 = \dfrac{1}{T_C}(u - x_4) \\ y = x_1, \end{cases} \tag{26}$$

where $K$, $T_1$, $T_2$, $T_3$, $T_C$ and $\alpha$ are system parameters, and $g(\boldsymbol{x}, u) = \frac{1}{T_1 T_2}[-x_2 - \alpha x_2^3 - (T_1 + T_2)x_3 + \frac{K(T_C - T_3)}{T_C} x_4 + \frac{K T_3}{T_C} u]$. In the form of (3), $f_d(\boldsymbol{x}, d(t), t) = d(t) - \frac{\alpha x_2^3}{T_1 T_2}$, $\boldsymbol{A}$, $\boldsymbol{B}$, $\boldsymbol{C}$ and $\boldsymbol{D}$ are denoted as follows:

$$\boldsymbol{A} = \begin{bmatrix} 0 & 1 & 0 & 0 \\ 0 & 0 & 1 & 0 \\ 0 & -\frac{1}{T_1 T_2} & -\frac{T_1 + T_2}{T_1 T_2} & \frac{K(T_C - T_3)}{T_1 T_2 T_C} \\ 0 & 0 & 0 & -\frac{1}{T_C} \end{bmatrix},$$

$$\boldsymbol{B} = \begin{bmatrix} 0 \\ 0 \\ \frac{K T_3}{T_1 T_2 T_C} \\ \frac{1}{T_C} \end{bmatrix}, \boldsymbol{C} = \begin{bmatrix} 1 & 0 & 0 & 0 \end{bmatrix}, \boldsymbol{D} = \begin{bmatrix} 0 \\ 0 \\ 1 \\ 0 \end{bmatrix}.$$

The control objective is to make the heading approach the predefined heading. The model and simulation parameters are set as: $K = 0.5900$, $T_1 = 0.9526$, $T_2 = 0.0247$, $T_3 = 0.2215$, $\alpha = 0.0001$, $T_C = 0.1000$, and $d(t) = -1.237 - -0.1t - 0.2t^2$ with $q = 2$. To guarantee the convergence of the discrete SCESO, the observer gain is chosen as $\boldsymbol{L}_{fc} = [1.7, 95.0, 3.3 \times 10^3, 822.0, 2.3 \times 10^5, 3.0 \times 10^6, 2.8 \times 10^7]^{\mathrm{T}}$ such that the eigenvalue magnitudes of $\boldsymbol{A}_{fc}^e$ and $\boldsymbol{A}_{fc}^g$ are both $[0.75, 0.73, 0.73, 0.69, 0.69, 0.65, 0.65]^{\mathrm{T}}$ satisfying Assumptions 2 and 3. The MPC parameters are set as: $N_P = 20$, $\boldsymbol{Q} = \mathrm{diag}[10^5, 10^2, 10^2, 10^2]$, $R = 1$ for (16), and the sample time for discretization and control $T_s = 0.1$ s. The objective output, i.e., objective heading, is $\psi_o = 20°$, and the objective states $\boldsymbol{x}_o$ are set as $[20, 0, 0, 0]^{\mathrm{T}}$ accordingly. The constraints for system states and input is set as $-30° \leqslant \tilde{x}_4(k+i) \leqslant 30°$, $-30° \leqslant \tilde{u}(k+i-1) \leqslant 30°$, $-20° \cdot T_s \leqslant \Delta\tilde{u}(k+i-1) \leqslant 20° \cdot T_s (-20°/s \leqslant \dot{u}(t) \leqslant 20°/s)$. The initial states of the real dynamics and observer are both $\boldsymbol{x}(0) = [0, 0, 0, 0]^{\mathrm{T}}$.

*6.2.2. Results*

The real, estimated value and observer error of states and the system input during the simulation are shown in Fig. 8.

From Fig. 8, it can be observed that the heading of vessel approaches the objective value, i.e., 20° and keeps constant after time $t = 6$ s, and the estimated values of heading rate and heading acceleration all converge to $\boldsymbol{0}$. It shows that the simulation results satisfy the Assumption 3. The observer errors of all states converge to $\boldsymbol{0}$ after $t = 5$ s even though the magnitude of external disturbances grows.

To verify the advance of this proposed method, a PID controller is applied to realize the same control objective with the same constraints as this is the most commonly used industry controller. After tuning, the coefficients for the proportional, integral, and derivative terms are set as $K_p = 4$, $K_i = 1$ and $K_d = 2$, respectively. Generally, it is difficult to tune the PID parameters to obtain good performance because the steady-state error is hardly corrected by adding an integral term while the disturbances are always changing. The comparison of the control performance of PID and proposed method is shown in Figs. 9 and 10.

From Fig. 9, it can be observed that the proposed controller tracks the objective heading after $t = 6$ s while the PID controller tracks the objective heading after $t = 16$ s with a small tracking error. The $summation\, of\, absolute\, error(20\,\mathrm{s}) = 41.1621$ for the proposed controller is much smaller than the $summation\, of\, absolute\, error(20\,\mathrm{s}) = 87.5993$ for the PID controller. From Fig. 10, the inputs with the proposed controller are smaller than inputs with the PID controller, which means that the proposed controller takes less energy.

## 7. Conclusions and future research

Considering that unmeasurable states and external disturbances usually exist in dynamic systems, it is difficult to control these systems without the information of system states and external disturbances, especially in the presence of system nonlinearities. To acquire accurate state information and attenuate the effect of disturbances is important to improve control performance. A state-compensation extended state observer based model predictive control method is proposed to obtain better control performance. The lumped disturbances encompassing external disturbances and neglecting system nonlinear terms are handled separately. The external disturbances are attenuated by extending states and system nonlinear terms are compensated by the estimated states simultaneously. The simulation experimental results show that the proposed method has the advantages of improving the tracking precision and speeding up the tracking error convergence. The stability of state-compensation extended state observer is analyzed theoretically and verified by numerical data. The path following control of autonomous vessels in the presence of wind, current and waves could be solved with the proposed control method when certain states are unknown or with large measurement errors.

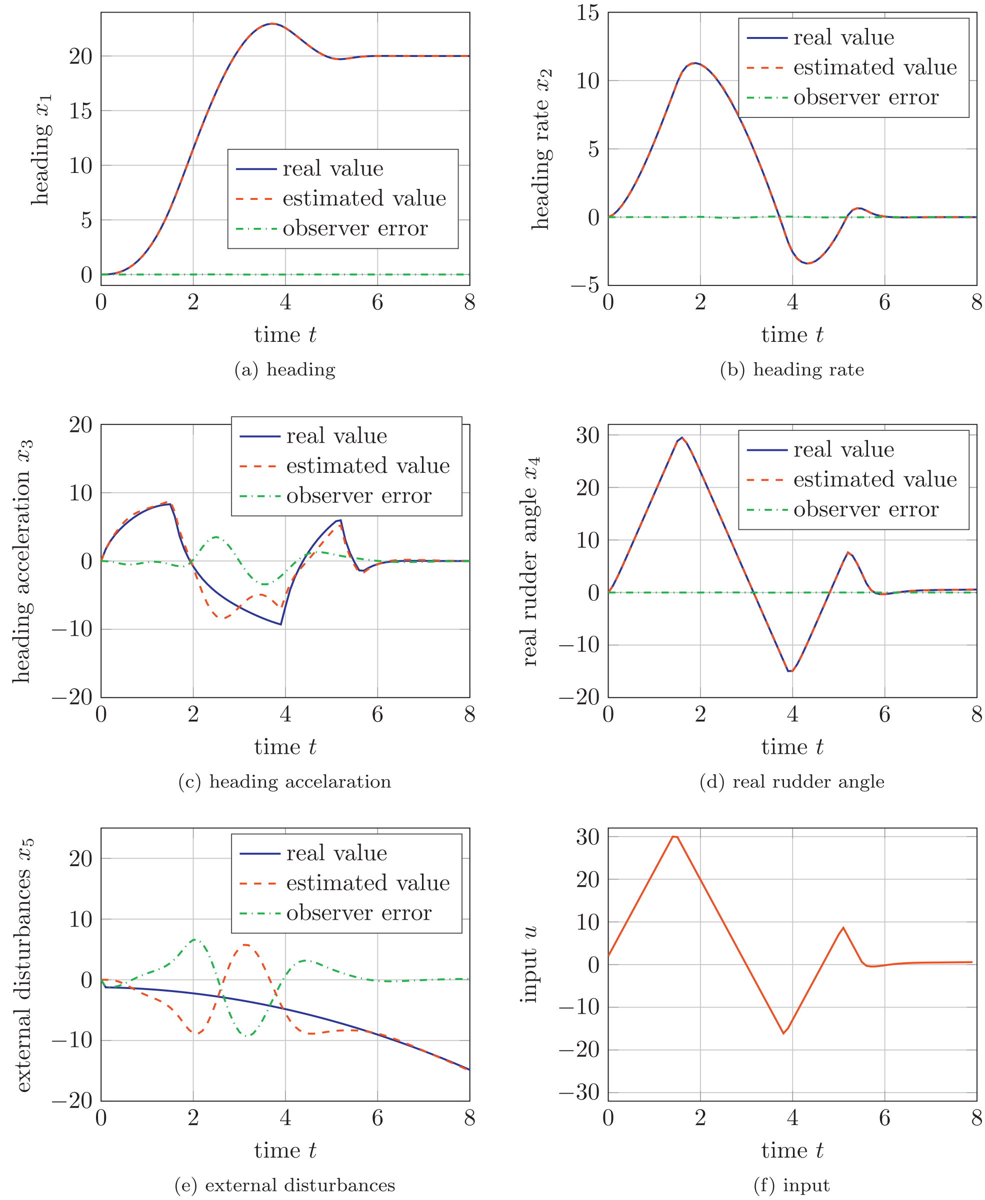

(a) heading
(b) heading rate
(c) heading accelaration
(d) real rudder angle
(e) external disturbances
(f) input

**Fig. 8.** The real, estimated value and observer error of states and input value.

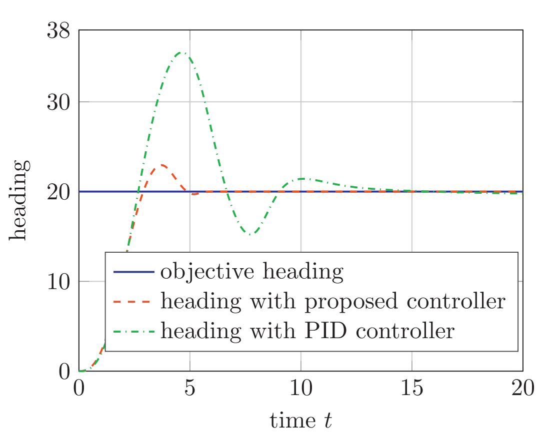

**Fig. 9.** The heading of proposed and PID controller.

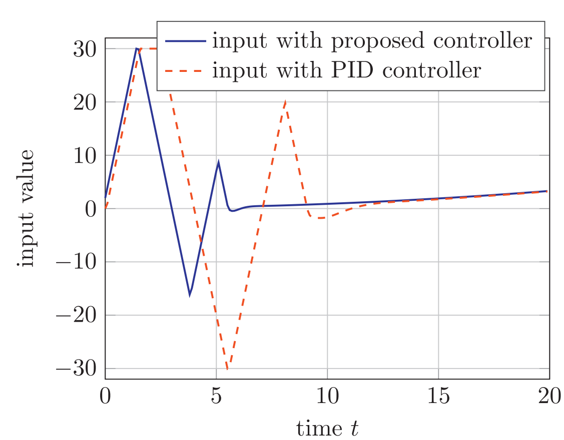

**Fig. 10.** The input value.

A control system with time delay, i.e., nonminimum-phase delay system, could have significant impact on control performance [47]. Therefore, future work will consider applying the improved extended state observer in the nonminimum-phase delay system.

## Acknowledgment

This research is supported by the China Scholarship Council under Grant 201506950053, the National Natural Science Foundation of China (NSFC) Project (No. 61273234), the Natural Science Foundation of Hubei Province Project (No. 2015CFA111), and the Project of Ministry of Transport, China (No. 2015326548030).

## References

[1] W. Caharija, K.Y. Pettersen, A.J. Sørensen, M. Candeloro, J.T. Gravdahl, Relative velocity control and integral line of sight for path following of autonomous surface vessels: merging intuition with theory, J. Eng. Marit. Environ. 228 (2) (2014) 180–191.
[2] E.F. Camacho, C. Bordons, Model Predictive Control, Springer, 2007.
[3] C.T. Chen, Linear System Theory and Design, Oxford University Press, Oxford, United Kingdom, 1995.
[4] J. Chen, R.J. Patton, H. Zhang, Design of unknown input observers and robust fault detection filters, Int. J. Control 63 (1) (1996) 85–105.
[5] W.H. Chen, D.J. Ballance, P.J. Gawthrop, J.J. Gribble, J. O'Reilly, A nonlinear disturbance observer for two link robotic manipulators, in: Proceedings of the 38th IEEE Conference on Decision and Control, volume 4, Phoenix, USA, 1999, pp. 3410–3415.
[6] W.H. Chen, J. Yang, L. Guo, S. Li, Disturbance-observer-based control and related methods–an overview, IEEE Trans. Ind. Electron. 63 (2) (2016) 1083–1095.
[7] M.S. Fadali, A. Visioli, Digital Control Engineering: Analysis and Design, Academic Press, United States, 2012.
[8] L.B. Freidovich, H.K. Khalil, Performance recovery of feedback-linearization-based designs, IEEE Trans. Autom. Control 53 (10) (2008) 2324–2334.
[9] Z. Gao, Scaling and bandwidth-parameterization based controller tuning, in: Proceedings of the American Control Conference, Colorado, USA, 2003, pp. 4989–4996.
[10] Z. Gao, Active disturbance rejection control: a paradigm shift in feedback control system design, in: Proceedings of the 2006 American Control Conference, Minneapolis, USA, 2006, pp. 2399–2405.
[11] Z. Gao, Y. Huang, J. Han, An alternative paradigm for control system design, in: Proceedings of the 40th IEEE Conference on Decision and Control, Florida, USA, 2001, pp. 4578–4585.
[12] B. Guo, Z. Z, On the convergence of an extended state observer for nonlinear systems with uncertainty, Syst. Control Lett. 60 (6) (2011) 420–430.
[13] J. Han, The extended state observer for a class of uncertain plants, Control Decis. 10 (1) (1995) 85–88.
[14] J. Han, From PID to active disturbance rejection control, IEEE Trans. Ind. Electron. 56 (3) (2009) 900–906.
[15] C.D. Johnson, Optimal control of the linear regulator with constant disturbances, IEEE Trans. Autom. Control 13 (4) (1968) 416–421.
[16] H. Khalil, Nonlinear Systems, Pearson, 2002.
[17] K.S. Kim, K.H. Rew, S. Kim, Disturbance observer for estimating higher order disturbances in time series expansion, IEEE Trans. Autom. Control 55 (8) (2010) 1905–1911.
[18] S.K. Kim, C.R. Park, T.W. Yoon, Y.I. Lee, Disturbance-observer-based model predictive control for output voltage regulation of three-phase inverter for uninterruptible-power-supply applications, Eur. J. Control 23 (2015) 71–83.
[19] S. Li, J. Yang, W. Chen, X. Chen, Generalized extended state observer based control for systems with mismatched uncertainties, IEEE Trans. Ind. Electron. 59 (12) (2012) 4792–4802.
[20] Z. Li, J. Sun, S.R. Oh, Design, analysis and experimental validation of a robust nonlinear path following controller for marine surface vessels, Automatica 45 (7) (2009) 1649–1658.
[21] H. Liu, S. Li, Speed control for PMSM servo system using predictive functional control and extended state observer, IEEE Trans. Ind. Electron. 59 (2) (2012) 1171–1183.
[22] D.Q. Mayne, J.B. Rawlings, C.V. Rao, P.O.M. Scokaert, Constrained model predictive control: stability and optimality, Automatica 36 (6) (2000) 789–814.
[23] R. Miklosovic, A. Radke, Z. Gao, Discrete implementation and generalization of the extended state observer, in: Proceeding of the 2006 American Control Conference, Minneapolis, USA, 2006, pp. 2209–2214.
[24] M. Morari, J.H. Lee, Model predictive control: past, present and future, Comput. Chem. Eng. 23 (4) (1999) 667–682.
[25] S.R. Oh, J. Sun, Path following of underactuated marine surface vessels using line-of-sight based model predictive control, Ocean Eng. 37 (2) (2010) 289–295.
[26] S.J. Ovaska, S. Valiviita, Angular acceleration measurement: a review, in: Proceedings of the 1998 IEEE Conference on Instrumentation and Measurement Technology, Minnesota, USA, 1998, pp. 875–880.
[27] R.J. Patton, J. Chen, Optimal unknown input distribution matrix selection in robust fault diagnosis, Automatica 29 (4) (1993) 837–841.
[28] R.J. Patton, J. Chen, Observer-based fault detection and isolation: robustness and applications, Control Eng. Pract. 5 (5) (1997) 671–682.
[29] J.B. Rawlings, Tutorial overview of model predictive control, IEEE Control Syst. 20 (3) (2000) 38–52.
[30] J. She, M. Fang, Y. Ohyama, H. Hashimoto, M. Wu, Improving disturbance-rejection performance based on an equivalent-input-disturbance approach, IEEE Trans. Ind. Electron. 55 (1) (2008) 380–389.
[31] J.J.E. Slotine, J.K. Hedrick, E.A. Misawa, On sliding observers for nonlinear systems, J. Dyn. Syst. Meas. Control 109 (3) (1987) 245–252.
[32] Y. Su, B. Duan, C. Zheng, Y. Zhang, G. Chen, J. Mi, Disturbance-rejection high–precision motion control of a Stewart platform, IEEE Trans. Control Syst. Technol. 12 (3) (2004) 364–374.
[33] B. Sun, Z. Gao, A DSP-based active disturbance rejection control design for a 1-kW H-bridge DC-DC power converter, IEEE Trans. Ind. Electron. 52 (5) (2005) 1271–1277.
[34] M.S. Tavazoei, Notes on integral performance indices in fractional-order control systems, J. Process Control 20 (3) (2010) 285–291.
[35] S.A. Velardi, H. Hammouri, A.A. Barresi, In-line monitoring of the primary drying phase of the freeze-drying process in vial by means of a Kalman filter based observer, Chem. Eng. Res. Des. 87 (10) (2009) 1409–1419.
[36] S. Vichik, F. Borrelli, Solving linear and quadratic programs with an analog circuit, Comput. Chem. Eng. 70 (2014) 160–171.
[37] Dan D. Wang, K.Y. Lum, Adaptive unknown input observer approach for aircraft actuator fault detection and isolation, Int. J. Adapt. Control Signal Process. 21 (1) (2007) 31–48.
[38] D. Wu, K. Chen, X. Wang, Tracking control and active disturbance rejection with application to noncircular machining, Int. J. Mach. Tools Manuf. 47 (15) (2007) 2207–2217.
[39] Y. Xia, Z. Zhu, M. Fu, Back-stepping sliding mode control for missile systems based on an extended state observer, IET Control Theory Appl. 5 (1) (2011) 93–102.
[40] J. Yang, S. Li, X. Chen, Q. Li, Disturbance rejection of dead-time processes using disturbance observer and model predictive control, Chem. Eng. Res. Des. 89 (2) (2011) 125–135.
[41] J. Yang, W. Zheng, S. Li, B. Wu, M. Cheng, Design of a prediction-accuracy-enhanced continuous-time MPC for disturbed systems via a disturbance observer, IEEE Trans. Ind. Electron. 62 (9) (2015) 5807–5816.
[42] J. Yang, W.X. Zheng, Offset-free nonlinear MPC for mismatched disturbance attenuation with application to a static VAR compensator, IEEE Trans. Circuits Syst. II: Express Briefs 61 (1) (2014) 49–53.
[43] M. Zeitz, The extended Luenberger observer for nonlinear systems, Syst. Control Lett. 9 (2) (1987) 149–156.
[44] A. Zemouche, M. Boutayeb, G.I. Bara, Observers for a class of Lipschitz systems with extension to hperformance analysis, Syst. Control Lett. 57 (1) (2008) 18–27.
[45] H. Zheng, R.R. Negenborn, G. Lodewijks, Predictive path following with arrival time awareness for waterborne AGVs, Transp. Res. Part C: Emerg. Technol. 70 (2016) 214–237.
[46] Q. Zheng, L. Gao, Z. Gao, On stability analysis of active disturbance rejection control for nonlinear time-varying plants with unknown dynamics, in: Proceedings of the IEEE Conference on Decision and Control, New Orleans, USA, 2007, pp. 12–14.
[47] P. Zhou, T. Chai, J. Zhao, DOB design for nonminimum-phase delay systems and its application in multivariable MPC control, IEEE Trans. Circuits Syst. II: Express Briefs 59 (8) (2012) 525–529.